

Competition between spin glass order and strong coupling superconductivity in a single - species fermion model

H. Feldmann and R. Oppermann
Institut für Theoretische Physik,
Univ. Würzburg, D-97074 Würzburg, FRG
 (December 31, 2021)

The phase diagram of a single species fermion model allowing for local pairing superconductivity (SC) and spin glass order (SG) is derived as a function of chemical potential μ and ratio $r \equiv v/J$ between attractive coupling v and frustrated magnetic interaction J . For ratios larger than a characteristic $r_c(\mu)$, superconductivity does not allow for SG order, while for smaller values a very detailed phase diagram arises with entangled spin glass and superconducting transitions. Our results for the Green's functions show that superconductivity occurring in the magnetic interaction band is of gapless type with a crossover from strongly gapless, within a certain range below T_c , to very weakly gapless in a wide low temperature regime, and hardgapped at $T = 0$.

PACS numbers: 71.27.+a, 74.25.Dw, 75.10.Nr

Phase diagrams of HighTcSuperconductors (HTS) have been reported which show a spin glass phase in between the antiferromagnetic and superconducting ones [1–4]. Strontium doped HTS are the most prominent examples, where antiferromagnetism gives way to clear signatures of spin glass (SG) like behaviour before superconductivity sets in at higher (hole)-doping. A typical SG order parameter was identified at moderately low temperatures $T < 8K$ [1] and even an infiltration within the superconducting domain at lowest temperatures was described [2]. Classes of HTS exist as well, which do not seem to show spin glass and/or intermediate phase, or it might have been impossible to detect it up to now. Existence and nature of intermediate spin glass or SG-alike phases in a certain doping range must be expected to be important features of strongly correlated systems. Experiments revealing close relations between magnetism and superconductivity in heavy fermion (HF) systems addressed coexistence, phase separation, and pairbreaking of local pairs by frozen moments for example [4,6]. Most of recent theories for HTS materials focussed on the destruction of antiferromagnetism under doping. Viewing an intermediate phase from the superconducting side, the appealing concept of a nodal liquid [7] was developed, leaving aside the notion and role of quenched disorder and randomness. Since we wish to deal here with superconductivity transitions under participation of a spin glass, a disorder model is a natural choice. Arguments on an important role of disorder in HTS and in HF-systems were provided experimentally and by theoretical reasoning [4–6]. Aspects such as non Fermi liquid behaviour, seen to arise in the vicinity of spin glass order [8], also support this point of view.

In this Letter we present detailed results for spin glass to superconductor transitions in a single-species fermionic model, which treats frustrated magnetic- and attractive interaction on the same footing. Unique features of the

phase diagram are derived analytically and numerically. We shall observe that for certain interaction ratios the location of the spin glass bears resemblance to that of a logarithmic resistivity regime residing above a spin glass ordered phase at lower T in Sr-doped HTS [5]. A fluctuational state of broken down spin glass order should contribute to transport properties seen in intermediate phases above T_f . In particular, SG-order was recently shown to affect transport properties strongly [9], an effect that due to the random interaction can well have a weak localization precursor.

We consider here a model described by the Hamiltonian $\mathcal{H} \equiv \mathcal{H}_{Jv} + \mathcal{H}_t$, where $\mathcal{H}_{Jv} = -\frac{1}{2} \sum J_{ij} \sigma_i \sigma_j - \sum v_{ij} a_{i\downarrow}^\dagger a_{i\uparrow}^\dagger a_{j\uparrow} a_{j\downarrow} - \mu \sum n_i$, $\mathcal{H}_t = \sum_{ij\sigma} t_{ij} a_{i\sigma}^\dagger a_{j\sigma}$, and $\sigma = n_\uparrow - n_\downarrow$, $a_{i\sigma}$, and $n = n_\uparrow + n_\downarrow$ denoting spin-, fermion-, and fermion-number operators respectively. The variance J^2 of the frustrated and Gaussian-distributed magnetic interaction J_{ij} and its magnitude relative to that of the attractive coupling, $v_{q=0}/J$, are relevant parameters of our analysis below, together with the chemical potential and the related filling factor $\nu(\mu)$. We restrict the discussion to the small t/J regime, which implies that the selfconsistently determined magnetic band is much larger than the hopping bandwidth in general. Only deep within the superconducting regime, where the magnetic bandwidth almost shrank to zero, the single fermion hopping bandwidth becomes dominant. Local pairs can be delocalized due to finite range v_{ij} and/or by arbitrarily weak fermion hopping t_{ij} . We employ a local pairing theory of superconductivity based on the order parameter $\Delta \equiv \langle a_{i\uparrow}^\dagger a_{i\downarrow}^\dagger \rangle$ and on a two-particle coherence length replacing the usual one-particle length in the corresponding Ginzburg-Landau theory. One-fermion Green's functions [10] are local as in the $d = \infty$ method [11,12]. Superconductivity is of Bose condensation type and crosses over into BCS type behaviour (not considered here) in the limit of small ratios between v and hopping bandwidth.

The phase diagram illustrated in Figures 1 and 2 is obtained from the free energy for model \mathcal{H}_{Jv} given by

$$f = \frac{1}{4}\beta J^2((\tilde{q}-1)^2 - (q-1)^2) + \frac{|\Delta|^2}{v} - T \int_{-\infty}^{\infty} \frac{dz}{\sqrt{2\pi}} e^{-z^2/2} \ln \mathcal{C}, \quad (1)$$

where $\mathcal{C} \equiv \cosh(\beta\tilde{H}) + \cosh(\beta\sqrt{|\Delta|^2 + \mu^2}) \exp(-\frac{1}{2}\beta J^2\chi)$ with $\chi = \beta(\tilde{q} - q)$ and effective field $\tilde{H} \equiv J\sqrt{qz}$; the saddle point solutions q , \tilde{q} , and Δ are found from the coupled selfconsistent equations obtained by extremizing f . The physical solutions of these coupled equations are not easy to identify, even outside the SG-phase; multiple solutions exist and changeovers of stability occur as chemical potential μ , temperature T , or interaction ratio v/J are varied. This leads to the complexity of the phase diagram displayed in Figures 1 and 2.

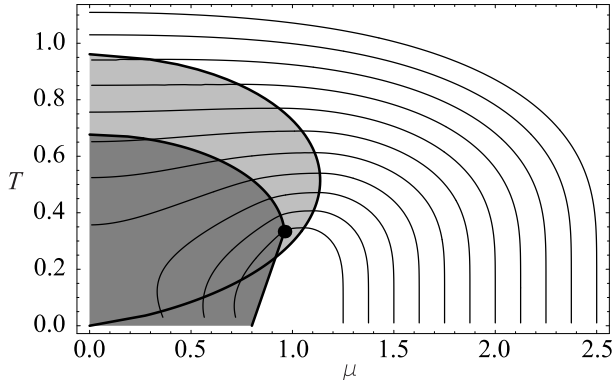


FIG. 1. Phase diagram of competing spin glass (SG) and superconducting (SC)-transitions (thin lines) for various attractive couplings v (given by $v = 2J\mu_{e.p.}$ at lines' right endpoint ($T = 0, \mu = \mu_{e.p.}$)), at fixed $J = 1$, and as a function of chemical potential μ (dark grey area: maximum SG-domain for $v = 0$). Thin lines enclose SC-phase which remove pieces of the ($v = 0$) SG-phase or suppress it totally at large enough v/J . The bold line l_3 delimiting the light grey area joins tricritical points (T_c -maxima) on SC-critical curves locating 1st order transitions left of l_3 .

Figures 1 and 2 reveal unique features of the competition between SG- and SC-order. For example, an enhanced fermion concentration $\nu(\mu)$ reduces the effective spin density at larger $|\mu|$ and is seen to suppress the spin glass stronger than it eliminates the superconducting phase as $\nu(\mu) \rightarrow 0$ or 2. Within a large region above the SG-phase, the SC-critical curves become deformed, as Fig.1 shows for $v/J < 4.5$, due to the increasing spin glass fluctuations fed by the random magnetic interaction. As the critical SC-curve passes through a maximum and starts to descend with decreasing μ , the SC-transitions change from second to first order. For still smaller ratios v/J the SC-line enters the $v = 0$ SG-phase: in this case, magnetic moments freeze first and a discontinuous SG-SC transition follows at lower temper-

ature (shown for $v/J = 3.25, 3.5, 3.75$). For still smaller v/J the 1st order SC-line falls rapidly to zero and the SG-phase prevents superconducting order up to a critical value μ_c (see $v/J = 3, 2.75, 2.5$). The replica symmetric solution also reveals the possibility of reentrant SC to SG-transitions, shown for $v/J = 2.5, 2.75, 3$ in Figure 1.

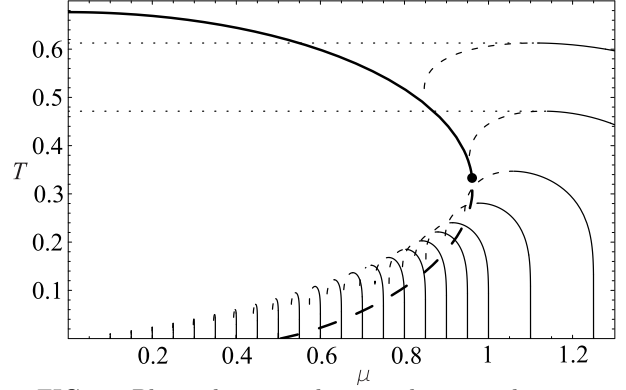


FIG. 2. Phase diagram close to the spin glass transition (bold line: pure SG-transition, bold-dashed line: paramagnetic stability limit) showing the stability limits of the superconducting (SC) phase (dotted horizontal lines, given only for $v/J = 3.5, 3.0$) and of the non-SC phase (dashed thin lines) bifurcating at SC-tricritical points. SC-critical (continued thin) lines are shown down to small v/J .

Figure 2 complements Figure 1 by adding, within a magnification of the SG-SC boundary, the stability limits of the superconductor and displays second order SC-transition lines crawling into the phase separation regime of the Ising spin glass for small v/J and T . For $T \rightarrow 0$, the quantum Parisi phase must be expected, which means that the paramagnetic stability limit should be shifted to the left. Lacking the full Parisi solution for $\mu > 0$ we employ numerical solutions of fermionic TAP-equations [13,14] to arrive at a straight line estimate of the discontinuous paramagnet-SG transition curve. Discontinuous SC-SG transitions for $\frac{v}{J} < 2.5$ must occur in between this curve and the SC-SG transition at $\frac{v}{J} = 2.5$. It is currently not possible to obtain a precise position of these discontinuous transitions at low T , since this would require to unite the dynamic mean field theory with the Parisi solution at infinite replica symmetry breaking (RSB) (despite the discontinuity, one step RSB is insufficient at and near $T = 0$). An estimate can be obtained from the few percent rise of the SG-energy due to RSB [15]. Furthermore, we arrive at the following conclusions:

- i) There is no coexistence of spin glass - and local pairing superconducting order parameter in zero magnetic field. The detailed analysis of the free energy and of all stability conditions shows only SC-SG transitions between $\{q \neq 0, \Delta = 0\}$ and $\{q = 0, \Delta \neq 0\}$ for $H = 0$.
- ii) The transition between the two phases is always discontinuous and exists only within a certain range of

chemical potentials (or filling).

iii) For large enough v/J , like $v/J > 4.13$ at half-filling for example, the spin glass is prevented by the superconducting transition, which is continuous for $v/J > 4.55$ at half-filling; below this value it becomes discontinuous. The tricritical line, which separates these domains is included in Figure 1 for several values of v/J and as a function of the chemical potential.

iv) Decreasing the temperature at fixed $\mu < .96$ (see Figure 1), a second transition from SG to superconductivity occurs at $T_c < T_f(v = 0)$. Figures 1 and 2 display the exact numerical results of the replica symmetric theory. It is known that the spin glass free energy increases a few percent as an effect of replica symmetry breaking, which should slightly enlarge the superconducting domain (these corrections increase with decreasing temperature). Recalling the change of the spin glass-ferromagnetic boundary under RSB [16] the reentrant behaviour from superconductor to spin glass and back to superconductor may disappear as well, but the SC-SG boundary will not become a vertical line (unlike the boundaries between SG and ferro- or antiferromagnetic phase in a purely magnetic model [16];

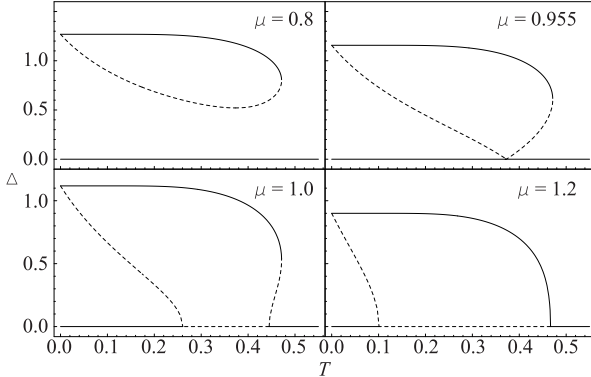


FIG. 3. Selfconsistent solutions for the superconducting order parameter Δ (continued lines), shown for $v/J = 3, q = 0$ and various μ values. Unstable solutions (dashed lines, maxima of f) explain stability limits and different discontinuous scenarios arising for sufficiently small μ .

Figure 3 shows the effect of random magnetic fluctuations, described by $\tilde{q}(T, \mu)$, on the superconducting order parameter for exemplary values of μ and $v/J = 3$. The absence of coexistent order parameters allows to set $q = 0$. For $\mu = 0.8$ a first order transition from $\Delta = 0$ to SC order occurs at a temperature below the tricritical $T_3 = 0.475J$, the latter being independent of μ . For $\mu = J$, the first order transition still occurs, but in addition the non-SC phase becomes locally unstable between the two zeros of the finite Δ solutions. At low temperatures, $\Delta = 0$ is locally stable again, but the global minimum remains at $\Delta \neq 0$. Beyond the tricritical point, $\mu > \mu_3(\frac{v}{J} = 3) = 1.14J$ in Figure 3, the stable SC solution continuously decreases to $\Delta = 0$.

In a magnetic field new aspects arise: the transition temperature of the superconductor will be reduced and finally vanish for $H > H_{c2}$, leaving a smeared spin glass transition for sufficiently small chemical potential. The overlap parameter q is nonzero in a field and then coexists with Δ , since the field can penetrate the present type II superconductor partially. In this case the Almeida Thouless line can enter the superconductor, infiltrating ergodicity breaking there.

We analyze the superconducting phase by means of the Green's functions: we derive the normal one $\mathcal{G}(\epsilon_n)$, the anomalous one $\mathcal{F}(\epsilon_n)$, and relevant particle-hole- $\Pi_{ph}(\omega_m)$ and particle-particle bubble diagrams $\Pi_{pp}(\omega_m)$ for various limits. Superconductivity arising in the magnetic band much larger than the hopping band is described by the (local) anomalous Green's function

$$\mathcal{F}(\epsilon) = \frac{i \Delta \exp(\beta^2 \tilde{q}/2)/(8\tilde{q}r_1)}{\cosh(\beta r_1) + \exp(\beta^2 \tilde{q}/2)} \quad (2)$$

$$\sum_{\{\lambda, s\}=\pm 1} (\epsilon + i\lambda r_1 + is\beta\tilde{q}) \mathcal{U}\left[1, \frac{3}{2}, \frac{(\epsilon + i\lambda r_1 + is\beta\tilde{q})^2}{2\tilde{q}}\right] + \frac{i \Delta \cosh(\beta r_1)/(4\tilde{q}r_1)}{\cosh(\beta r_1) + \exp(\beta^2 \tilde{q}/2)} \sum_{\lambda \pm 1} (\epsilon + i\lambda r_1) \mathcal{U}\left[1, \frac{3}{2}, \frac{(\epsilon + i\lambda r_1)^2}{2\tilde{q}}\right]$$

where $r_1 \equiv \sqrt{\mu^2 + \Delta^2}$, $\epsilon \equiv (2n+1)\pi T$, $J = 1$, \mathcal{U} denotes the hypergeometric U-function (Kummer function) [17], and the SC order parameter obeys $\Delta = vT \sum_{\epsilon} \mathcal{F}(\epsilon)$.

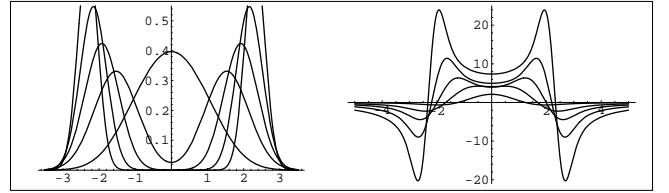


FIG. 4. Density of states $\rho(E)$ (left) and $\text{Re}\{\mathcal{F}(E)\}$ (right), for $(v = 5J, \mu = 0, T_c \approx 1.11J)$ and real energies E , show crossover from strongly to weakly gapless superconductivity for decreasing temperatures $T/J = 1.1, 1.0, .9, .8$ and $.7$

The solution for $\mathcal{G}(\epsilon)$, being similarly given in terms of the Kummer function, yields the density of states plotted together with $\text{Re}\{\mathcal{F}\}$ in Figure 4 (weak fermion hopping and dynamic corrections from $\Pi_{ph}(\omega)$ and $\chi(\omega)$ are negligible here). These plots of course employ the stable selfconsistent solutions for $\tilde{q}(T, \mu)$ and $\Delta(T, \mu)$ inserted in (2). They demonstrate the crossover from strongly gapless superconductivity just below T_c to a pronounced pseudogap. Although invisibly small for temperatures lower than roughly 20% below T_c , the density of states remains nonzero in the pseudogap regime and vanishes there only at $T = 0$. The term gapless superconductor should be used with care, since over a wide temperature range the gap looks almost perfect. The rounding of the superconducting gap edges and the retarded

way it opens up below T_c is reminiscent of the magnetic gap found below spin glass transitions [9]. As the superconducting gap sharpens at lower T , the magnetic band narrows and eventually the fermion hopping (bandwidth) starts to dominate. Then the anomalous Green's function crosses over into the hopping band solution which we derived for gaussian random t_{ij} as

$$\mathcal{F}(\epsilon) = -\frac{\Delta}{2w^2} + \frac{\Delta}{\sqrt{2}w^2} \frac{\sqrt{w^2 + \epsilon^2 + \Delta^2 - \mu^2 + r(\epsilon)}}{\sqrt{\epsilon^2 + \Delta^2}}, \quad (3)$$

where $r(\epsilon) = \sqrt{4w^2(\epsilon^2 + \Delta^2) + (-w^2 + \epsilon^2 + \Delta^2 + \mu^2)^2}$ with $w^2 \equiv 4\langle t_{ij}^2 \rangle$. Equation (3) is an exact local solution which holds for arbitrary bandwidth w and chemical potential μ , extending an earlier result for half-filling [10]. The transition temperature derived from (3) illustrates in Figure 5 the crossover from linear Bose condensation $T_c(v)$ -dependence to exponential BCS-type.

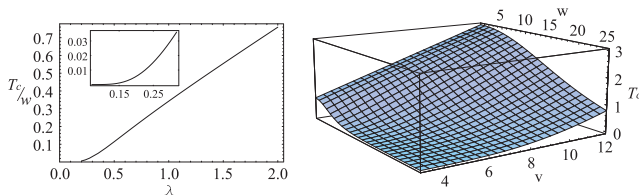


FIG. 5. Complete crossover from Bose condensation type to BCS behaviour illustrated in 3D plot of $T_c(v)$ as w/v increases; typical values for both linear and exponential dependence are given as a function of $\lambda \equiv v\rho_F$

The Bose-BCS crossover can be followed through the whole parameter range due to the local property of the one-particle Green's functions, a feature appreciated as well in the $d = \infty$ method for clean systems [11,12]. The suppression of one particle phase coherence, due to infinite dimensions in clean systems or by symmetry requirement in the quenched average used here, results in type II superconductivity with two particle coherence length replacing the standard one in the Ginzburg Landau theory (many details including paramagnetic pairbreaking were published in [10]) The puzzling coexistence phenomena in zero field, absence of $(q \neq 0, \Delta \neq 0)$ solutions but presence of phase separation regimes, and the related discontinuous transition between the magnetic and superconducting phases is further elucidated by the bubble diagram $\Pi_{pp}(T, \omega)$. At half-filling for example, the condition $1 = v\Pi_{pp}(T_c, \omega = 0)$ yields $T_c = (1 - \tilde{q}(T_c))\frac{v}{4}$, ($\tilde{q} = T\chi|_{\omega=0}$). Equating this with the spin glass freezing temperature $T_f = J\tilde{q}(T_f)$, ie solving formally $T_c = T_f$ to search for simultaneous onset of both types of order, results in $\tilde{q} = v/(v + J)$. Since $\tilde{q}(T_f) = .6767$ one finds $v = 4.1862$ (let $J = 1$). Since $\max\{\Pi(T, \mu = 0, \omega = 0)\} = .242$ at $T = .731$ no solution exists for $v < v_{\min} = 4.14$, while two solutions are found for $v = 4.186 > v_{\min}$, only those with $T > .731$ being free energy minima. At half-filling, the thermal first

order superconducting transition occurs at temperature $T_{c1} > T_f$ for $v > 3.8$, but the stability limit of the normal phase is absent for $3.8 < v < 4.14$; spin glass order will not reappear down to lowest temperatures. For $v < 3.8$ the spin glass transition occurs at $T_f = .6767$ with a first order SG-SC transition to follow at lower temperature.

For the sake of transparency we discussed only fully frustrated magnetic interactions and zero field phenomena. Subsequent antiferromagnetic-spin glass-superconductor transitions, as μ increases from zero are not simply obtained once the J_{ij} is given an antiferromagnetic part. Thus, models extended by the Hubbard interaction, but also the allowance for different symmetries of the order parameter, and the dynamic quantum Parisi phase are examples for future research on links between antiferromagnetism, spin glass order, and superconductivity.

The model we analyzed here proved to have a special type of gapless superconductivity due to the vicinity of spin glass order and due to correlations induced by the frustrated magnetic interaction.

We acknowledge support by the DFG under grant Op28/5-1 and by the SFB410.

-
- [1] F. C. Chou, N. R. Belk, M. A. Kastner, R. J. Birgeneau, and A. Aharony, Phys. Rev. Lett. **75**, 2204 (1995)
 - [2] D. J. Scalapino, Phys. Rep. **250**, 329 (1995)
 - [3] W. Brenig, Phys. Rep. **251**, 155 (1995)
 - [4] J. A. Mydosh, J. Magn. Magn. Mat. **157/158**, 606 (1996)
 - [5] I. Korenblit, V. Cherepanov, A. Aharony, and O. Entin-Wohlmann, cond-mat/9709056
 - [6] H. Spille, M. Winkelmann, U. Ahlheim, C. Bredl, F. Steglich, P. Haen, J. Migot, J. Thoulence, and R. Tournier, J. Magn. Magn. Mat. **76/77**, 539 (1988) and references therein
 - [7] L. Balents, M.P.A. Fisher, C. Nayak, cond-mat/9803089
 - [8] A. Georges and A. Sengupta, Phys. Rev. **B52**, 10295 (1995)
 - [9] R. Oppermann and B. Rosenow, Phys. Rev. Lett. **80**, 4767 (1998) and to appear in Phys. Rev. **B** (1998)
 - [10] R. Oppermann, Physica **A167**, 301 (1990) and references therein
 - [11] D. Vollhardt in *Correlated electron systems*, World Scientific, 57 (1994)
 - [12] A. Georges, G. Kotliar, W. Krauth, and M. Rozenberg, Rev. Mod. Phys. **68** 13 (1996).
 - [13] D.J. Thouless, P.W. Anderson, and R.G. Palmer, Phil. Mag. **35**, 593 (1977)
 - [14] M. Rehker and R. Oppermann, cond-mat/9806092
 - [15] G. Parisi, J. Phys. **A13**, 1101 (1980)
 - [16] K. Binder, A.P. Young, Rev. Mod. Phys. **58**, 801 (1986)
 - [17] M. Abramovitz and I. Stegun, Handbook of Mathematical Functions, Dover Publ. Inc, NY (1965)
 - [18] B. Rosenow and R. Oppermann, Phys. Rev. Lett. **77** 1608 (1996)